ACS OMEGA

http://pubs.acs.org/journal/acsodf

Article

Investigating the Effect of a Diesel–Refined Crude Palm Oil Methyl Ester–Hydrous Ethanol Blend on the Performance and Emissions of an Unmodified Direct Injection Diesel Engine

Jarernporn Thawornprasert, Wiriya Duangsuwan, and Krit Somnuk*

Cite This: *ACS Omega* 2023, 8, 9275–9290

Read Online

ACCESS | Metrics & More | Article Recommendations

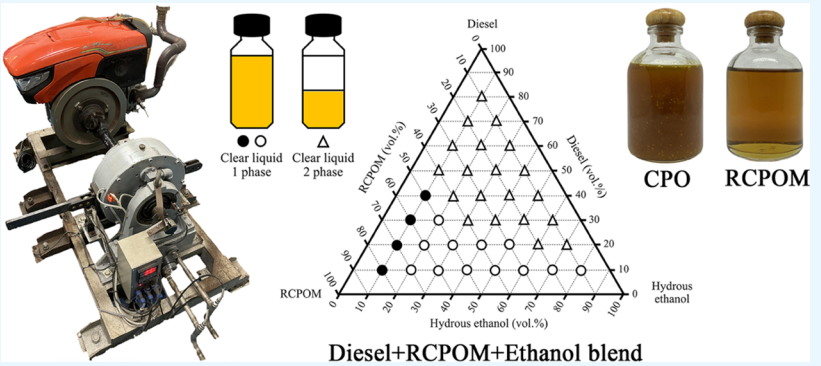

ABSTRACT: In this research, the optimum condition for the production of refined crude palm oil methyl ester from refined crude palm oil was investigated using the response surface method via the transesterification reaction in a batch process. The refined crude palm oil was obtained by vacuum distillation of crude palm oil to extract some of the free fatty acids from the oil, providing nutritional benefits and reducing the chemical consumption of the production process. The purity of methyl ester in the refined crude palm oil methyl ester was studied to adjust four independent variables: methanol content (11–23 vol %), concentration of potassium hydroxide (4–12 g/L), stirrer speed (100–500 rpm), and reaction time (9–45 min). The results showed that methyl ester had a purity of 96.91 wt % when synthesized under optimal conditions of 18.2 vol % methanol, a potassium hydroxide concentration of 10.0 g/L, a stirring speed of 380 rpm, and a reaction time of 36.4 min at 60 °C. Refined crude palm oil methyl ester was blended with diesel and ethanol to study the feasibility of using the diesel–refined crude palm oil methyl ester–hydrous ethanol blend in an unmodified diesel engine. A comparative study of fuel properties, emissions, and performance of the diesel–refined crude palm oil methyl ester–ethanol blend was used to assess the feasibility of fuel blends (D40RM50E10, D30RM60E10, D20RM70E10, and D10RM80E10) in diesel engines at various engine speeds and loads. The results showed that the D40RM50E10 blend provided the closest performance to diesel and was environmentally friendly, as it provided nitrogen oxide and carbon monoxide emissions 32 and 55% lower than those with diesel, respectively. The test results indicated that the diesel–refined crude palm oil methyl ester–hydrous ethanol blend is an attractive alternative fuel in agricultural engines that reduces diesel consumption and benefits farmers and rural communities.

1. INTRODUCTION

Several countries have used petroleum fuels to reinvigorate and develop their economies in industries such as manufacturing, power generation, agriculture, and transportation, resulting in scarcity and higher prices of petroleum resources.[1] However, an increase in the usage of petroleum fuels has increased the level of air pollution.[2] Therefore, environmental issues are unavoidable as the global usage of petroleum fuels increases. Biofuels such as diesohol and biodiesel have emerged as liquid fuels that can reduce emissions from diesel engines.[3,4] As an alternative fuel, diesohol is produced by blending diesel with ethanol.[5] Ethanol is commonly used as a component because it can be produced from wastes and crops such as corn, sugarcane, cassava, and molasses.[6−8] Blending ethanol with diesel has many advantages, owing to a high oxygen level and a high latent heat of vaporization of ethanol, which improves complete combustion in diesel engines. It also reduces the concentrations of NO_x, CO,

Received: November 24, 2022
Accepted: February 23, 2023
Published: March 3, 2023

and particulate matter (PM) and lowers combustion temperatures.[9,10] Many studies have reported that a straight blending of 95 vol % hydrous ethanol in diesel engines is not advised. Although hydrous ethanol (95 vol %) is less pure than anhydrous ethanol (99.9 vol %), hydrous ethanol is cheaper. When residual water in hydrous ethanol is removed using the molecular sieve dehydration process, high energy consumption and manufacturing costs are required.[11,12] Some studies have reported the addition of hydrous ethanol to a fuel blend, and owing to the high concentration of oxygenates in these fuel blends, they can be used in diesel engines to reduce emissions.[13−15] However, since ethanol is a polar molecule and diesel contains nonpolar molecules, polar molecules dissolve in polar solvents. Likewise, nonpolar molecules dissolve in nonpolar solvents according to the solubility rule (like dissolves like). As a result, adding a high concentration of ethanol to diesel is difficult, particularly at low temperatures.[16] The blending of ethanol into diesel has limited solubility, which results in poor fuel stability. To solve the problem of the stability of the mixture, biodiesel is recommended as an emulsifier to prevent the phase separation between diesel and ethanol. Since biodiesel contains both lipophilic and hydrophilic parts, it is suitable to be used as an emulsifier to prevent the phase separation of fuel blends. Therefore, biodiesel is used as an emulsifier to maintain the stability of diesel−biodiesel−ethanol fuel blends. Biodiesel can also reduce NO_x, CO, CO_2, hydrocarbon (HC), and PM emissions that impact the environment.[19−21]

As aforementioned, the addition of high-concentration ethanol affects the solubility performance of diesel, resulting in low blending phase stability.[4,17,22,23] However, by blending diesohol with biodiesel, this issue may be resolved. Because biodiesel is a fatty and hydrophilic fuel with a structure comparable to that of diesel and ethanol, Subbaiah et al.[17] used it as an emulsifier in a phase separation solution of diesohol. Khoobbakht et al.[22] reported that ethanol can be blended with biodiesel in any ratio, but it cannot be blended with diesel. The addition of ester as an additive enhances the solubility of diesohol, resulting in increased fuel stability. Jin et al.[23] reported similar results and confirmed that the hydrophobicity of diesel fuel is the primary cause of the instability of the ternary system, which includes diesel−biodiesel−ethanol blends. The stabilities of diesel and ethanol improve when the biodiesel content is higher. Several research studies have reported that ethanol concentrations of >15 wt % should not be blended with diesel to avoid phase separation. The engine performance may be negatively affected by the addition of ethanol due to changes in fuel characteristics (heating value, viscosity, density, low cetane number, ignition delay, and automatic ignition).[2,24−26] Shrivastava et al.[24] reported that adding ethanol decreases the density, viscosity, and heating value of fuel blends. Additionally, the cetane number of the mixture decreases with the addition of ethanol because ethanol has a low cetane number between 5 and 8, resulting in poorer ignition. Srikanth et al.[25] reported similar results and concluded that an increase in ethanol concentration over 15% leads to a decrease in cetane number, delaying ignition. Pidol et al.[2] reported anomalous autoignition characteristics in the blended fuels when 20% ethanol was added to the blended fuels. Kumar et al.[26] found that adding more than 20% ethanol to fuel blends reduces thermal efficiency because of the low temperature in the combustion chamber. Jamrozik et al.[27] tested diesel−biodiesel−ethanol blends at a constant engine speed at 70, 85, and 100% of the engine load to determine the effect of engine load on engine emission and performance. A small amount of ethanol added to a blended fuel can decrease its viscosity and density, which leads to improvements in fuel spray and combustion. Klajn et al.[28] studied the performance and emissions of the diesohol fuel blend in a generator diesel engine. They found that the efficiency of the engine was acceptable at an ethanol concentration of <10%, reducing NO_x emissions. Krishna et al.[29] reported similar results, explaining that the cooling effect of ethanol reduces NO_x emissions at low loads but significantly increases NO_x emissions at maximum loads owing to higher temperatures in a cylinder. Additionally, the increased oxygen content from the addition of biofuels contributes to the complete fuel combustion in the engine, resulting in lower CO emissions than those observed with diesel. Alternatively, complete combustion promotes higher CO_2 emissions. Shamun et al.[30] reported that high oxygen concentrations in the fuel mix result in up to 52% combustion efficiency at high loads. Conversely, Kaulani et al.[31] reported that HC and CO emissions were higher than those with diesel at low loads owing to the high oxygen content in the blends. Tan et al.[32] increased the concentrations of ethanol by 0, 5, 10, and 15 vol % in diesel−biodiesel−ethanol blends tested in diesel engines. They concluded that when the concentration of ethanol ranged from 0 to 15 vol %, the brake thermal efficiency (BTE) and brake-specific fuel consumption (BSFC) were 20−42% and 0.4−0.5 kg/kWh, respectively. Krishna et al.,[29] Kaulani et al.,[31] and de Oliveira et al.[33] reported that increasing the concentration of ethanol in the fuel decreased BTE and increased BSFC for a maximum ethanol content of 15% when compared to diesel. Freitas et al.[34] found that adding 10% ethanol to a diesel−biodiesel−ethanol blend reduced torque and brake power (P_b) by 6%. However, the thermal efficiency of each fuel was not considerably different.

In Thailand, crude palm oil (CPO) was used as the potential raw material in the production of commercial biodiesel. A major problem of the biodiesel production process is the concentration of free fatty acid (FFA) in CPO because a >1 wt % FFA concentration in oil causes saponification, which converts lipids into soaps through a base catalyst, leading to poorer biodiesel yields.[35,36] The production of biodiesel from high-FFA oil was carried out via a two-stage process.[37] In the first step, FFA in oil was converted to an ester using the esterification reaction with an acid catalyst. In the second step, the esterified oil was then converted to triglycerides, which were then converted into ester and glycerol via the transesterification reaction with a base catalyst.

However, many studies have reported the nutritional and cosmetic value of FFA.[38] It is used as a raw material for manufacturing various products in the animal feed, soap, and oleochemical industries. FFAs are also a source of vitamin E, phytosterols, and squalene, which are valuable substances for dietary supplement and cosmetic industries.[39,40] Before producing biodiesel from CPO, valuable FFAs should be refined from CPOs that contain a high concentration of FFAs by a physical refining process. Herein, refined CPO (RCPO) from vacuum distillation was studied to reduce FFA contents in CPO using a physical refining process before it was used as feedstock for biodiesel production. According to many researchers, the main issue with using a direct blend of petroleum diesel and vegetable oil in diesel engines is the high viscosity that results from the composition of vegetable oil. RCPO is converted to methyl ester (ME) by a two-stage process for mixing in the diesel−hydrous ethanol blend. Furthermore, several studies

https://doi.org/10.1021/acsomega.2c07537
ACS Omega 2023, 8, 9275−9290

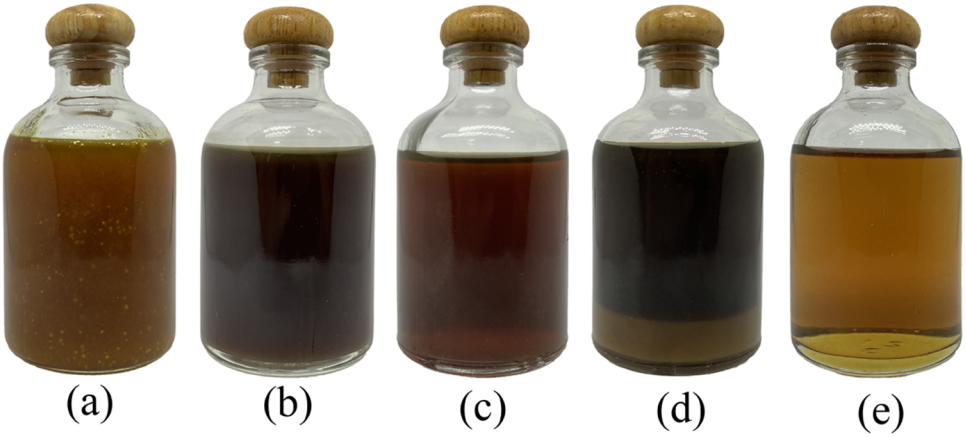

Figure 1. Raw materials and products from esterification and transesterification processes: (a) CPO, (b) RCPO, (c) ERCPO, (d) crude RCPOM, and (e) RCPOM.

Table 1. Properties of Raw Materials and Chemicals Used in Biodiesel Production of RCPO

		for esterification			for transesterification		
property	CPO[44]	RCPO[44]	methanol	H_2SO_4	ERCPO[44]	methanol	KOH
density@60 °C (kg/L)	0.885	0.884	0.753	1.798	0.882	0.753	
viscosity@60 °C (cSt)		22.52	0.35		17.66	0.35	
boiling point (°C)			64.7	330		64.7	1327
purity (%)			99	98		99	95
ester (wt %)					2.278		
TG (wt %)	86.170	93.526			96.289		
DG (wt %)	2.845	0.304			0.405		
MG (wt %)	0.300						
FFA (wt %)	10.685	6.170			1.028		

have suggested that ethanol should not be directly blended with diesel. However, the price of anhydrous ethanol is higher than that of hydrous ethanol. To improve the stability and properties of hydrous ethanol blending in diesohol, biodiesel from RCPO was used as an emulsifier to produce fuel blends. Thus, the goal of this study is to fulfill a research gap in biodiesel production from RCPO using a two-stage procedure. Four independent factors, namely, methanol content (11−23 vol %), concentration of KOH (4−12 g/L), stirrer speed (100−500 rpm), and reaction time (9−45 min), were varied to produce high-quality MEs from esterified oils from RCPO using the response surface method (RSM) in a continuous transesterification process with a circulating hot water bath. Furthermore, the stability and properties of fuel blends of diesel, RCPO biodiesel, and ethanol were investigated and compared with those of diesel standards. Finally, the performance (P_b, BSFC, and BTE) and emissions (NO_x, CO, CO_2, O_2, and HC) of the fuel blend were compared with those of diesel to assess the feasibility of using the fuel blend at various engine speeds (1100−2300 rpm) and engine loads (25, 50, and 75%) in diesel engines without modification.

2. MATERIALS AND METHODS

2.1. Materials. The phase stability of diesel−refined crude palm oil ME (RCPOM)−hydrous ethanol was investigated using diesel B10 (10% ME with 90% diesel) from a filling station, and 95 vol % hydrous ethanol was purchased from a chemical sales company in Bangkok, Thailand. CPO with a high-FFA content was purchased from a palm oil mill. In the transesterification process for producing RCPOM, CPO was used as the initial feedstock for biodiesel production. The high FFA level in CPO was decreased to less than 1 wt % by an acid esterification process, followed by a base transesterification process. To remove some of the FFA in CPO and reduce chemical consumption in the esterification process, a vacuum refining technique was used. Additionally, the condenser used to distill some of the FFA in CPO contained nutritional advantages owing to its high content of essential FFA and carotene.[41−43] The final product of the vacuum refining process is known as RCPO, which is the product of a chemical-free CPO refining process using vacuum refining. The residual FFAs in the RCPO were then removed by the esterification reaction, a chemical process that converts FFA to ester. The final product from the esterification procedure is known as esterified refined crude palm oil (ERCPO). Thawornprasert et al.[44] reported the procedure for minimizing FFA content in ERCPO through esterification. The esterification reaction is shown in eq 1. The final step of the biodiesel production process, as shown in Figure 1, involves applying ERCPO as the raw material for the transesterification reaction. The transesterification reaction is shown in eq 2. The experiments used purely commercial-grade chemicals, including 98% potassium hydroxide (KOH) and 99% methanol. The properties of RCPO, ERCPO, and KOH are shown in Table 1.

$$\text{FFA} + \text{Alcohol} \xleftrightarrow{\text{Acid catalyst}} \text{Ester} + \text{Water} \quad (1)$$

$$\text{Triglycerides} + \text{Alcohol} \xleftrightarrow{\text{Base catalyst}} \text{Ester} + \text{Glycerol} \quad (2)$$

2.2. Optimization of Biodiesel Production from ERCPO. *2.2.1. Experimental Design.* Optimal ME purity in RCPOM during the second transesterification was determined

https://doi.org/10.1021/acsomega.2c07537
ACS Omega 2023, 8, 9275−9290

using the RSM. The effect of ME purity on the transesterification process was examined using a central composite design. Experiments of the five levels of −2, −1, 0, +1, and +2 were designed by varying the methanol content (11−23 vol %), concentration of KOH (4−12 g/L), stirrer speed (100−500 rpm), and reaction time (9−45 min). The factors and code levels are shown in Table 2, and the experimental design for 28 experiments is shown in Table 3. The purity of ME after transesterification was modeled using a second-degree polynomial and multiple regression, as shown in eq 3.[8]

Table 2. Independent Variables and Code Levels of RSM Experiments

		coded variable level				
independent variables	units	−2	−1	0	+1	+2
methanol (M)	vol %	11	14	17	20	23
KOH (K)	g/L	4	6	8	10	12
stirrer speed (S)	rpm	100	200	300	400	500
reaction time (T)	min	9	18	27	36	45

$$Y = \beta_0 + \sum_{i=1}^{k} \beta_i x_i + \sum_{i=1}^{k} \beta_{ii} x_i^2 + \sum_{i=1} \sum_{j=i+1} \beta_{ij} x_i x_j + \varepsilon \quad (3)$$

Table 3. Experimental Design and Purity of Methyl Ester Resulting from the Second Stage of the Transesterification Process[a]

experiments	M (vol %)	K (g/L)	S (rpm)	T (min)	ME (wt %)
1	11	8	300	27	91.86
2	14	6	200	18	93.04
3	14	6	200	36	93.91
4	14	6	400	18	94.65
5	14	6	400	36	94.90
6	14	10	200	18	96.22
7	14	10	200	36	97.18
8	14	10	400	18	97.44
9	14	10	400	36	98.09
10	17	4	300	27	94.02
11	17	8	100	27	97.12
12	17	8	300	9	96.51
13	17	8	300	27	98.81
14	17	8	300	27	98.49
15	17	8	300	27	98.78
16	17	8	300	27	98.53
17	17	8	300	45	99.04
18	17	8	500	27	98.26
19	17	12	300	27	99.21
20	20	6	200	18	96.54
21	20	6	200	36	97.24
22	20	6	400	18	96.87
23	20	6	400	36	98.51
24	20	10	200	18	98.39
25	20	10	200	36	98.58
26	20	10	400	18	98.54
27	20	10	400	36	98.55
28	23	8	300	27	97.64

[a]Notes: M, methanol; K, potassium hydroxide; S, stirrer speed; T, reaction time; ME, purity of methyl ester.

2.2.2. Experimental Procedure for Biodiesel Production from ERCPO. For preparing biodiesel, a circulating hot water bath was used to ensure the temperature of ERCPO was constant at 60 °C during the batch process of the transesterification reaction. ERCPO (400 mL) was poured into the reaction flask, and a six-bladed disk turbine was used to stir the mixture, and a mechanical agitator (IKA, model: RW 20 digital) was used to adjust the speed of the stirrer. Methanol and KOH were blended in a beaker using a magnetic stirrer to obtain a CH_3OK solution. Subsequently, the reaction was initiated by slowly adding potassium methoxide solution to the flask using a buret and counting the time immediately. Since the rapid addition of potassium methoxide solution increases the temperature of the reaction mixture, as it is an exothermic reaction, the temperature of the mixture was carefully controlled to ensure it did not exceed 64.7 °C (boiling point of methanol). For collecting samples, the reaction in the sample was stopped by rapidly cooling each sample in ice water. This was done to prevent the ME reaction from proceeding either forward or backward.[45] Crude biodiesel was purified to remove the remaining methanol and KOH after the transesterification reaction. Samples were washed using warm water until the hydrogen ion potential (pH) in the wastewater was 7. After the purification process, biodiesel was tested for ME, triglyceride (TG), FFA, diglyceride (DG), and monoglyceride (MG) using thin-layer chromatography with a flame ionization detector (TLC/FID, model: IATROSCAN MK-65; Mitsubishi Kagaku Iatron Inc., Tokyo, Japan).

2.3. Blending of Diesel−RCPOM−Hydrous Ethanol. The diesel−RCPOM−ethanol blend was produced using the following method: first, RCPOM was mixed with ethanol using a stirrer at 300 rpm for 5 min at 35 °C. Second, diesel was then poured into the mixture and stirred for 5 min to homogenize the three blend components. After mixing, the diesel−RCPOM−ethanol blend was kept in sealed bottles to prevent ethanol evaporation. The phases of diesel, RCPOM, and ethanol blends were physically observed for various diesel (10−80 vol %), RCPOM (10−80 vol %), and ethanol (10−80 vol %) concentrations, and the phases are shown in a ternary diagram in the section on phase stability of diesel−RCPOM−hydrous ethanol. Third, the phase behavior of all of the samples was monitored for 90 days at 35 °C. Lastly, the density and viscosity of the homogeneous fuel blend were studied according to diesel fuel specifications before testing in diesel engines.

2.4. Fuel Property Testing. The elemental analysis of organic substances in the fuel was conducted using a CHNS/O analyzer (model: Flash 2000, ThermoScientific, Italy) to determine the heating value of fuels. The pour and cloud points were measured using a Herzog CPP 97-2 instrument according to ASTM-D97[46] and ASTM-D2500,[47] respectively. The analytical methods for studying the composition of ME and linolenic acid ester in the fuel were based on EN-14103,[48] whereas the compositions of TG, MG, DG, total glycerin, and free glycerin in fuel were measured according to EN-14105.[49] Acid value levels of the esterified oils and biodiesel were examined by titration according to ASTM-D664-09.[50] The residual methanol contents in products were measured using gas chromatography (GC)-FID according to EN-14110.[51] The flash point was determined using the semiautomatic Pensky−Martens apparatus (model: Walter Herzog GmbH, Germany) in accordance with ASTM-D93-16a.[52] The physical properties of oils were determined according to ASTM-D1298-12b,[53] and a hydrometer was used to measure the density, and viscosity was

https://doi.org/10.1021/acsomega.2c07537
ACS Omega 2023, 8, 9275−9290

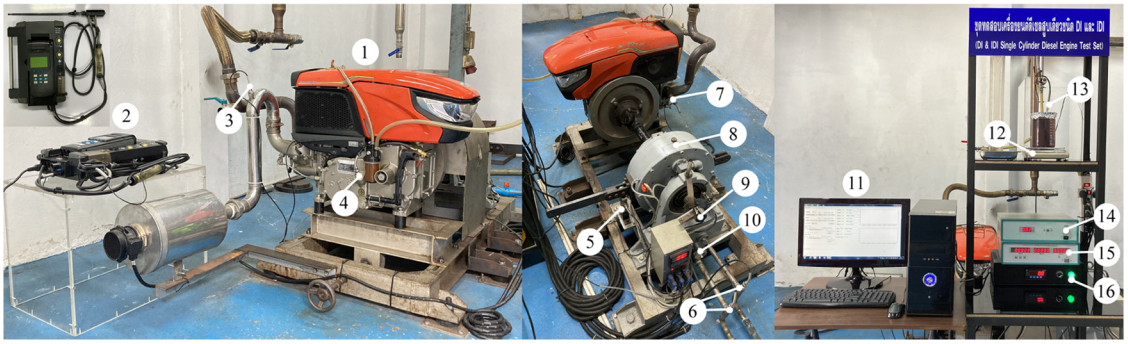

Figure 2. Diesel engine and dynamometer setup: (1) Kubota ZT100 DI, (2) emission analyzer, (3) air temperature sensor, (4) engine oil temperature sensor, (5) strain gauge load cell, (6) water temperature sensor, (7) exhaust gas temperature sensor, (8) dynamometer, (9) rotary encoder, (10) electric contact pressure gauge, (11) computer, (12) electronic digital scale, (13) fuel temperature sensor, (14) load controller, (15) instrument panel, and (16) data logger.

Table 4. Technical Specifications of the Test Engine and Dynamometer

engine characteristics	specification	dynamometer characteristics	specification
model	ZT100 DI	model	DW16
type of engine	4-stroke, cooling with water	type of dynamometer	eddy current brake
type of combustion	DI, direct injection	max. power	16 kW
method of charging	naturally aspirated	max. torque	70 Nm
number of cylinders	1	max. speed	13 000 rpm
cylinder arrangement	horizontal	turning inertia	0.02 kg·m^2
compression ratio	18:1	max. voltage	80 V
bore/stroke	88/90 mm	max. current	3.5 A
displacement volume	547 cm^3	cooling water pressure	0.02−0.05 MPa
max. power	7.35 kW, 2400 rpm	flow of cooling water	6.5 L/min
max. torque	33.34 Nm, 1600 rpm		
max. speed	2400 rpm		
injection timing	15−17° BTDC		
injection pressure	220 kg/cm^2		

measured using a Julabo MD-16G Visco Bath (Julabo Labortechnik GmbH, Seelbach, Germany) according to ASTM-D445-17a.[54] The water content and sediment were measured using a Coulometric Karl Fischer titrator (model: DL39, Mettler−Toledo Instrument. Inc., Greifensee, Switzerland) according to EN-ISO 12937[55] and ASTM-E203[56] methods, respectively. Copper strip corrosion was examined using a Herzog HZ9011 according to ASTM-D130-04.[57] Residual carbon in the fuel was analyzed by the ASTM-D4530 method.[58] The iodine value in biodiesel was determined using the Wijs technique and a GC-FID (model: GC 6850, Agilent Technologies) in accordance with EN-14111.[59] The sulfur, phosphorus, and sulfated ash contents were determined according to ASTM-D2622,[60] EN-14107,[61] and ASTM-D874,[62] respectively.

2.5. Diesel Engine Testing. *2.5.1. Measurements for Diesel Engine Testing.* The experiments on performance and emissions were performed using a single-cylinder, four-cycle engine; a direct-injected, compression ignition engine; and a water-cooled Kubota ZT100 DI diesel engine. Figure 2 shows the diesel engine and dynamometer experimental setup. The maximum compression ratio for the Kubota ZT100 DI diesel engine was 18:1, the maximum torque was 33.34 Nm at 1600 rpm, and the maximum speed was 2400 rpm. The engine was connected to the dynamometer (model: DW16, Jiangsu Lan Ling Test Equipment Co., Ltd., China) to simulate engine load for measuring the engine torque. The dynamometer had a maximum power of 16 kW, a maximum torque of 70 Nm, and a maximum speed of 13 000 rpm. A cooling water system with a centrifugal pump was used to cool the dynamometer. During the operation of the dynamometer, the water pressure in the cooling system was maintained between 0.0 and 0.4 MP, and the water output temperature must not be higher than 35 °C for the operation to be considered safe. The cooling of the dynamometer is important to ensure that the device prematurely deteriorates from the effects of shaft blocking, torque overload, and the insulation of the coils, generating the magnetic field. An engine load controller (model: SC-1D, 90 V, 5 A, Jiangsu Lan Ling Test Equipment Co., Ltd., China) was used to adjust the electrical current in the dynamometer to generate a magnetic field and adjust engine torque. An encoder (model: E6B2-CWZ6C, OMRON; Japan) was used to measure the shaft speed connected to the engine by the flywheel to observe and confirm the speed of the engine during operation. The force of the dynamometer was measured using an S-type beam load cell (model: RM-S2, Ruima Electric Manufacturing Co., Ltd., China), and the force from the load cell was then converted to torque (Nm). Data on the torque, engine speed, and engine power was shown on the instrument panel (model: CFY-2S, Jiangsu Lan Ling Test Equipment Co., Ltd., China). During testing, a data logger was used to collect data from the engine testing (power, torque, speed, and temperature of fuel, engine oil, exhaust gas, fresh air, and inlet and outlet water for cooling the dynamometer) in real time over a long period of time using multiple sensors. The diesel engine and dynamometer specifications are given in Table 4.

https://doi.org/10.1021/acsomega.2c07537
ACS Omega 2023, 8, 9275−9290

Table 5. Percentage Uncertainties of Various Instruments[a]

measurement parameter	measuring range	instrument	accuracy	uncertainty (%)
		Measured Variables		
O_2 (vol %)	0−25 vol %	emission analyzer	±0.8%	±0.06
CO (ppm)	0−10 000 ppm	emission analyzer	±5%	±0.02
CO_2 (vol %)	0−25 vol %	emission analyzer	±0.8%	±0.14
NO_x (ppm)	0−3000 ppm	emission analyzer	±5%	±0.01
HC (ppm)	0−40 000 ppm	emission analyzer	±10%	±0.22
EGT (°C)	0−1000 °C	temperature sensor	±2.6%	±1.00
engine speed (rpm)	0−6000 rpm	rotary encoder	±10 rpm	±0.20
fuel weight (g)	0−300 g	digital scale	±0.02 g	±0.01
time (s)		digital stopwatch timer	±0.1 s	±0.10
fuel temperature (°C)	−250 to 1300 °C	temperature sensor	±2.6 °C	±0.20
load (Nm)	0−70 Nm	strain gauge load cell	±0.1%	±0.01
LHV (kJ/kg)		CHNS/O analyzer		±0.80
		Calculated Parameters		
P_b[a] (W)				±0.21
fuel consumption[b] (kg/h)				±0.31
BSFC[c] (kg/kW·h)				±0.52
BTE[d] (%)				±1.32

[a]The uncertainty of P_b is [(uncertainty of engine speed) + (uncertainty of load)], is equal to [(0.2) + (0.01)] = ±0.21%. [b]The uncertainty of fuel consumption is [(uncertainty of fuel weight) + (uncertainty of time) + (uncertainty of fuel temperature)], is equal to [(0.01) + (0.1) + (0.2)] = ±0.31%. [c]The uncertainty of BSFC is [(uncertainty of P_b) + (uncertainty of fuel consumption)], is equal to [(0.21) + (0.31)] = ±0.52%. [d]The uncertainty of BTE is [(uncertainty of LHV) + (uncertainty of BSFC)], is equal to [(0.80) + (0.52)] = ±1.32%.

2.5.2. Uncertainty Analysis. To ensure the accuracy of the experimental results of the performance and gas emission characteristics of the diesel engine, uncertainty analysis was performed. The experimental range, accuracy, percentage of uncertainty, and measuring device are all described in Table 5. The lower heating value (LHV) acquired from the CHNS/O analyzer was utilized to compute the BTE uncertainty. As noted in the footnote of Table 5, the percentage uncertainties were calculated to be 0.21, 0.31, 0.52, and 1.32% for P_b, fuel consumption, BSFC, and BTE, respectively. The percentage of uncertainties from various instruments, including the rotary encoder, load cells, digital scale, digital stopwatch timer, temperature sensors, and CHNS/O analyzer, were used to estimate these percentages of uncertainties. The overall experimental performance and emission uncertainty for this study was defined as ±1.68% using the following equation

Overall experimental emission and performance uncertainty:

$$= (\text{uncertainty of } \{(O_2)^2 + (CO)^2 + (CO_2)^2 + (NO_x)^2 + (HC)^2 + (EGT)^2 + (BTE)^2\})^{1/2}$$

$$= (\text{uncertainty of } \{(0.06)^2 + (0.02)^2 + (0.14)^2 + (0.01)^2 + (0.22)^2 + (1)^2 + (1.32)^2\})^{1/2}$$

$$= \pm 1.68\%$$

3. RESULTS AND DISCUSSION

3.1. Prediction Model and Statistical Analysis of the RSM. According to the RSM, prediction models were developed to find the optimal conditions for ME production from ERCPO by evaluating the correlation between the independent and dependent parameters. The purity of ME produced from 28 tests ranged from 91.86 to 99.21 wt %, as shown in Table 3. A second-degree polynomial model was predicted for the production of ME from ERCPO. The influence of methanol concentration, KOH concentration, stirrer speed, and reaction time on ME purity was examined using complete multiple regression techniques at a 95% confidence level. Equation 4 shows the predicted model for the correlation between the purity of ME and the four parameters. The R^2 and $R_{adjusted}^2$ values of ME purity were 0.969 and 0.953, respectively. Table 6 shows the coefficients, *p*-value, and analysis of variance (ANOVA) for the regression correlating to ME production. The *p*-values of <0.05 for each coefficient were considered significant in the models. The terms $\beta_1 M$ and $\beta_6 M^2$ in eq 4 had the lowest *p*-value in the correlation prediction equation analysis. As a result, the methanol content considerably increased in the purity of ME in RCPOM for batch transesterification processes. The influence of the potassium hydroxide content was denoted by the terms $\beta_2 K$ and $\beta_7 K^2$, which ranked third and fourth,

Table 6. Values of coefficients and ANOVA of the Prediction Model[a]

coefficient	value	*p*-value
β_0	31.35	0.0000027357
β_1	4.668	0.000000000165532
β_2	3.893	0.000000139414
β_3	0.01724	0.00472
β_4	0.185	0.00606
β_5	−0.07844	0.000370
β_6	−0.107	0.00000000222092
β_7	−0.124	0.000024074
β_8	−0.0000226771	0.01895
β_9	0.00254	0.03122
R^2	0.969	
$R_{adjusted}^2$	0.953	

source	SS	MS	F_0	F_{signif}	DOF
regression	103.18	11.46	61.74	2.46 ($F_{0.05,9,18}$)	9
residual	3.342	0.186			18
total	106.53				27

[a]Note: SS is the sum of squares, MS is the mean square, F_0 is the ANOVA coefficient, F_{signif} is *F*-table of critical values at a significance level of 0.05, and DOF is the degrees of freedom.

https://doi.org/10.1021/acsomega.2c07537
ACS Omega 2023, 8, 9275−9290

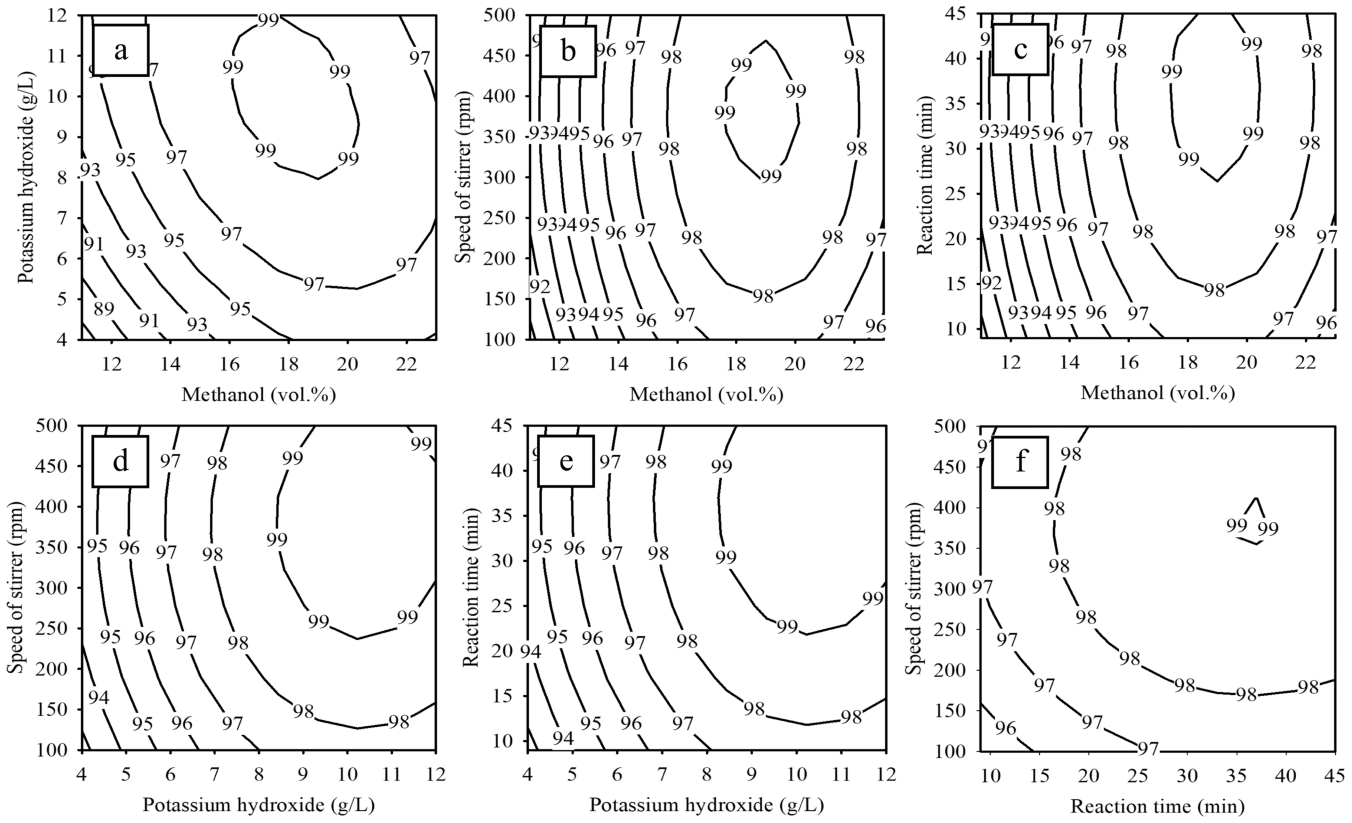

Figure 3. Contour plots of the effects of the four parameters on ME purity in RCPOM: (a) methanol and KOH contents, (b) methanol content and stirrer speed, (c) methanol content and reaction time, (d) KOH content and stirrer speed, (e) KOH content and reaction time, and (f) reaction time and stirrer speed.

Table 7. Properties of RCPOM

	result	biodiesel standard			
property	RCPOM	THA[a]	US[b]	EU[b]	for an agricultural engine in Thailand[a]
For Commercial Biodiesel Production					
ME (wt %)	96.91	96.5 min.		96.5 min.	
linolenic acid ester (wt %)	0.117	12.0 max.		12.0 max.	
density@15 °C (kg/m^3)	876	860−900		860−900	860−900
viscosity@40 °C (cSt)	4.5	3.5−5.0	1.9−6.0	3.5−5.0	1.9−8.0
flash point (°C)	154	120 min.	93 min.	101 min.	120 min.
carbon residue (wt %)	<0.1	0.3 max.	0.05 max.	0.3 max.	
water and sediment (vol %)	0.032 wt %	0.05 max.	0.05 max.	0.05 max.	0.2 max.
total contamination (mg/kg)		24 max.		24 max.	
copper strip corrosion	no. 1a	no. 1 max.	no. 3 max.	no. 1 max.	no. 3 max.
acid value (mgKOH/g)	0.37	0.50 max.	0.50 max.	0.50 max.	0.8 max.
iodine value (g iodine 100/g)	52.4	120 max.		120 max.	
methanol (wt %)	<0.01	0.2 max.	0.2 max.	0.2 max.	
TG (wt %)	0.2	0.2 max.		0.2 max.	
DG (wt %)	1.5	0.2 max.		0.2 max.	
MG (wt %)	0.37	0.7 max.		0.8 max.	
FFA (wt %)	0				
free glycerin (wt %)	0	0.02 max.	0.02 max.	0.02 max.	
total glycerin (wt %)	0.14	0.25 max.	0.24 max.	0.25 max.	0.02 max.
cetane number		51 min.	47 min.	51 min.	1.5 max.
phosphorus (wt %)	0.130	0.001 max.	0.001 max.	0.0004 max.	47 min.
sulfated ash (wt %)	0.05				0.02 max.

[a]From Somnuk et al.[8] [b]From Sajjadi et al.[63]

respectively. The *F*-test results at a 95% confidence level revealed that the F_0 value of 61.74 was greater than the F_{crit} value of 2.46 ($F_{0.05,9,18}$), as shown in Table 6. In terms of ME purity, the correlation prediction equation was statistically significant.

https://doi.org/10.1021/acsomega.2c07537
ACS Omega 2023, 8, 9275−9290

Table 8. Properties of Diesel (B10), RCPOM, Hydrous Ethanol, and Fuel Blends

				diesel−RCPOM−hydrous ethanol			
property	diesel (B10)	RCPOM	hydrous ethanol	D40RM50E10	D30RM60E10	D20RM70E10	D10RM80E10
density@15 °C (kg/m^3)	836	876	810	852	856	860	865
viscosity@40 °C (cSt)	2.54	4.50	1.16	3.01	3.18	3.37	3.57
cloud point (°C)		13					
pour point (°C)	<10[a]	12		3	4	6	8
sulfur (wt %)	<0.005[a]						
water content	<200 mg/kg[a]	0.03 wt %	5.00 vol %				
copper strip corrosion	<no. 1[a]	no. 1a					
oxidation stability	>35 h	54.27 min.					63 min.
carbon residue (wt %)	<0.03	<0.1					<0.1
flash point (°C)	>52[a]	154	18.5			room temperature	
high heating value (MJ/kg)	45.9	39.3	23.4	40.4	39.7	39.0	38.4
LHV (MJ/kg)	42.9	36.5	20.7	37.5	36.9	36.3	35.6
methyl esters	9−10 vol %[a]	96.91 wt %					

[a]Department of Energy Business.[68]

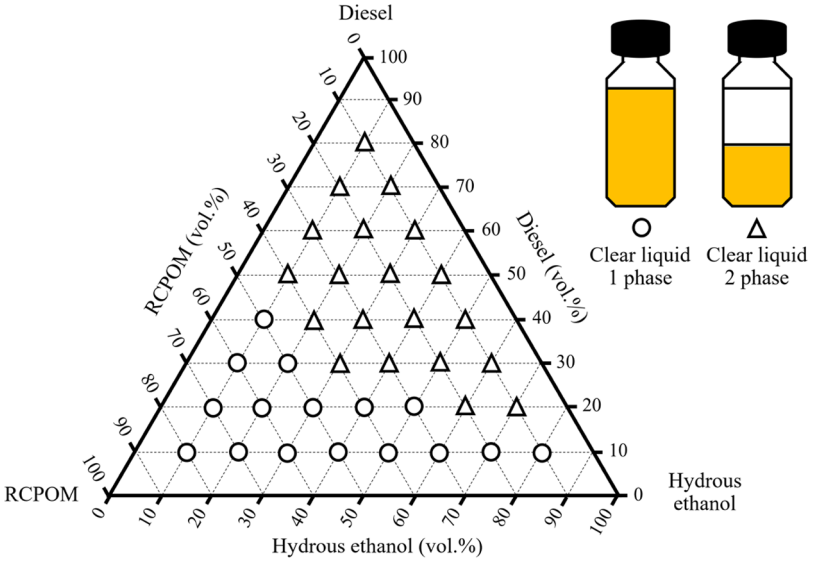

Figure 4. Long-term phase diagram of diesel−RCPOM−ethanol at room temperature; ○ represents the presence of a clear liquid single-phase system and Δ represents the presence of a clear liquid two-phase system.

$$\mathrm{ME} = \beta_0 + \beta_1 M + \beta_2 K + \beta_3 S + \beta_4 T + \beta_5 MK + \beta_6 M^2 + \beta_7 K^2 + \beta_8 S^2 + \beta_9 T^2 \quad (4)$$

where ME is the purity of methyl ester (wt %), M is the methanol content (vol %), K is the concentration of KOH (g/L), S is the stirrer speed (rpm), T is the reaction time (min), and β is the coefficient value.

3.2. Response Surface Plots and Optimal Conditions. Relationships between dependent and independent variables in ERCPO ME production are shown as contour plots in Figure 3. The maximum ME purity of 99.83 wt % was predicted under the optimal conditions of 18.2 vol % methanol, 10.0 g/L KOH, a stirrer speed of 380 rpm, and 36.4 min at 60 °C. The correctness of the model of ME purity was confirmed by the results of actual experiments, which demonstrated the optimal conditions for ensuring ME purity. Thus, in the actual experiment, 96.91 wt % ester was synthesized under optimum conditions. The compositions and physical properties of RCPOM compared to biodiesel specifications in the United States, the European Union, and Thailand are shown in Table 7.

3.3. Phase Stability of Diesel−RCPOM−Hydrous Ethanol. The properties of raw material fuels used in fuel blends are shown in Table 8. A ternary phase diagram was used to investigate the phase stability of the fuel blend at 35 °C. As shown in Figure 4, the phase behavior of fuel blends can be categorized into two types based on their physical characteristics: clear liquid in a single phase and in two phases. The clear liquid single-phase system is a homogeneous fuel blend with no separation of layers or suspended particles. The clear liquid two-phase system is a two-phase liquid system in which the two layers are clearly separated, and there are no suspended particles. The fuel blends were kept at 35 °C, and their stability was observed for 90 days. Note that the two clear liquid phases appeared within 1 day of blending RCPOM and diesel for samples in which the concentration of RCPOM was <40 vol %. Furthermore, the results showed that increasing the RCPOM content can improve the stability of the diesel−ethanol blend. Because RCPOM is biodiesel, it can be used as an emulsifier to combine ethanol and diesel.[2,18] Pidol et al.[2] and Shahir et al.[18] concluded that adding fatty acid ME into the diesel−ethanol blends improved the stable phase of fuel blends. Thus, when the

https://doi.org/10.1021/acsomega.2c07537
ACS Omega 2023, 8, 9275−9290

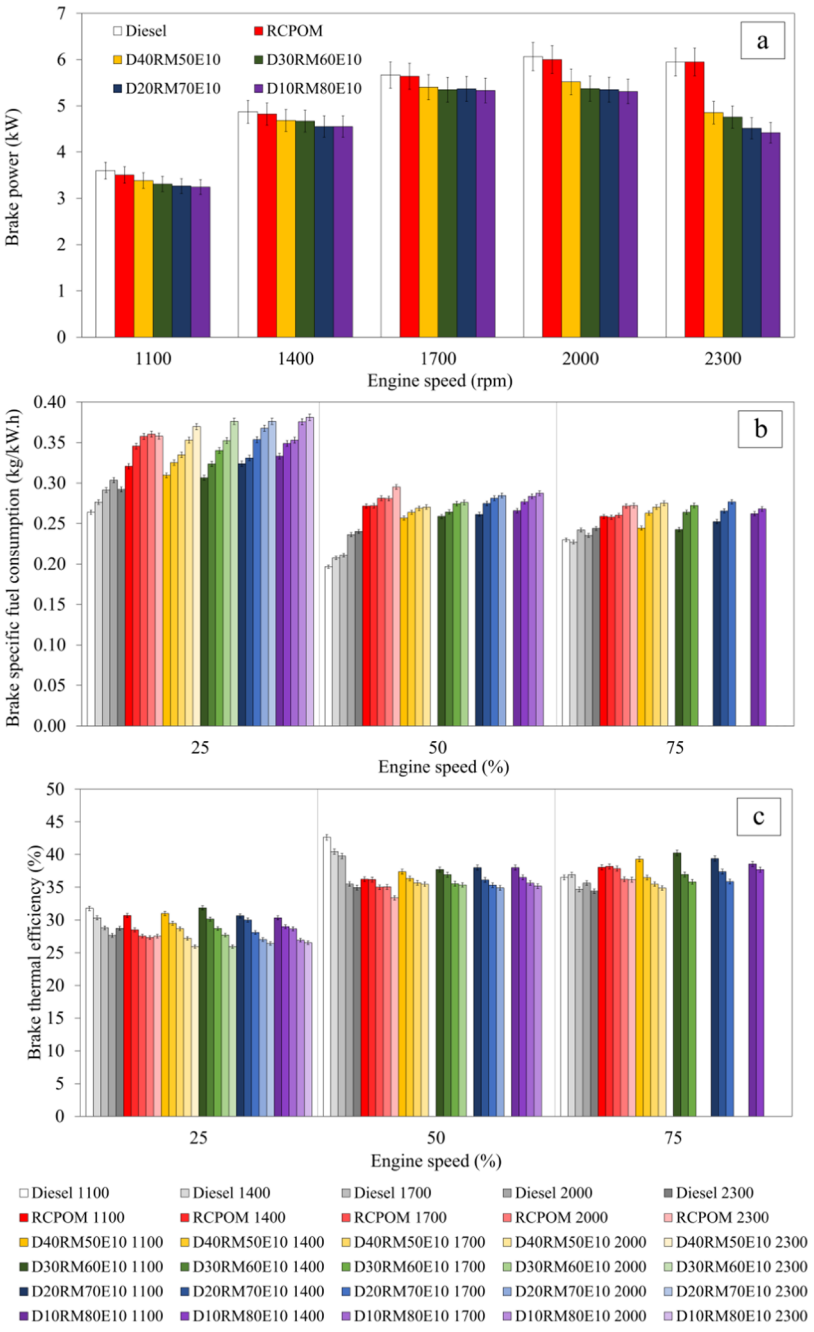

Figure 5. Effects of all fuels on the performance of diesel engines operating at various engine speeds and loads: (a) P_b, (b) BSFC, and (c) BTE.

concentration of RCPOM was >50 vol % and the concentration of diesel was <40 vol %, the clear liquid single phase appeared, and the fuel blend phase separation was not observed even after 90 days. Therefore, the density and viscosity were considered for the remaining 16 ternary blends (16 white dots). The viscosities of D10RM30E60, D10RM20E70, and D10RM10E80 blends were 1.75, 1.55, and 1.38 cSt at 40 °C, respectively. Therefore, the viscosity of these fuel blends did not conform to the standard requirements for diesel (1.8−4.1 cSt at 40 °C). Thus, remaining 13 blends were evaluated for testing in DI diesel engines. However, diesel engines should not be run with fuel blends that contain >15% ethanol without engine modification.[2,64−66] The excessive ethanol content in the fuel blend results in an unstable engine, vibration, and difficulty in controlling the engine.[67] Therefore, the NO_x, CO, CO_2, and HC emissions, O_2 gas emission, P_b, BSFC, and BTE of the engine for the outstanding four ternary blends of diesel−RCPOM−ethanol, namely, D40RM50E10, D30RM60E10, D20RM70E10, and D10RM80E10, were investigated in unmodified diesel engines running at various engine speeds and loads using a dynamometer. Table 8 shows the properties of diesel, biodiesel, ethanol, and fuel blends.

3.4. Engine Performance. *3.4.1. Brake Power.* Figure 5a shows the P_b for diesel, RCPOM, and fuel blends at different engine speeds. The P_b of all fuels increased as the engine speed increased up to 2000 rpm. The P_b of RCPOM is slightly lower than that of diesel at all speeds. The viscosity and density of biodiesel are higher than those of diesel, resulting in lower fuel combustion efficiency,[69] as shown in Table 8. Moreover, the LHV of biodiesel is also lower than that of diesel, resulting in

https://doi.org/10.1021/acsomega.2c07537
ACS Omega 2023, 8, 9275−9290

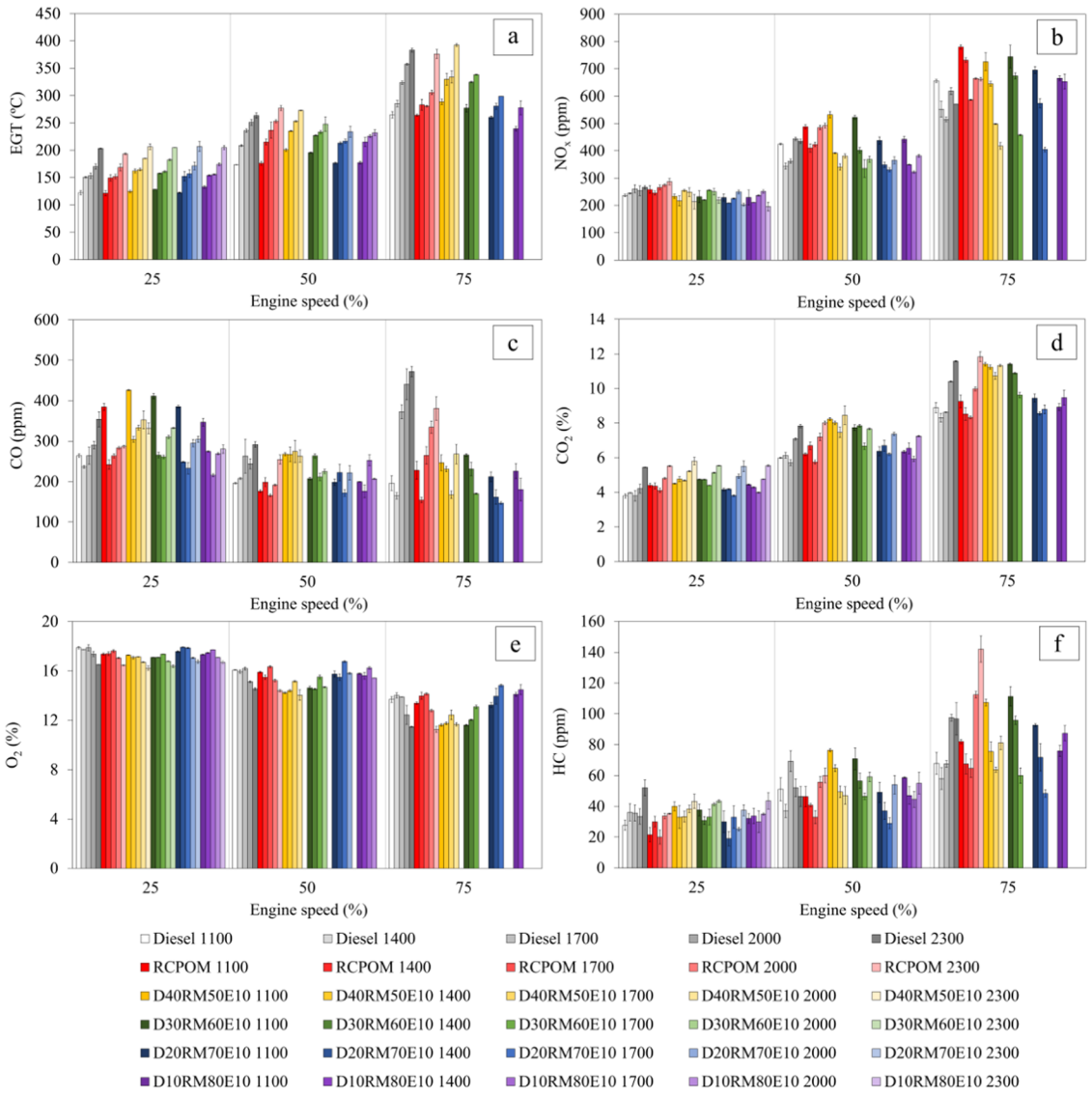

Figure 6. Effect of engine loading on the combustion of fuels in a diesel engine as measured using different emissions: (a) EGT, (b) NO_x, (c) CO, (d) CO_2, (e) O_2, and (f) HC.

lower P_b.[69] For all fuel blends, P_b increased as the engine speed increased from 1100 to 2000 rpm and decreased as the speed increased from 2000 to 2300 rpm. At all speeds, the P_b of the fuel blends was lower than that of diesel. Because ethanol has a lower cetane number and heating value than diesel, the P_b of fuel blends is lower than that of diesel at a maximum engine speed of 2300 rpm; the P_b values of D40RM50E10, D30RM60E10, D20RM70E10, and D10RM80E10 were 18.39, 20.12, 24.05, and 31.46%, respectively. Jia et al.[70] reported that the engine brake power of the diesel−biodiesel−ethanol blend was lower than that of diesel and decreased in proportion to the increase in biodiesel or ethanol content because the calorific value of the fuel blend was lower than that of diesel. Tripathi et al.[71] reported a similar result and stated that adding ethanol to the fuel blend led to reduced cetane numbers and engine power due to a longer ignition delay.

3.4.2. Brake-Specific Fuel Consumption. BSFC shows the fuel consumption in 1 h to produce 1 kW of brake power.[32] Figure 5b shows the variation in BSEC of diesel, RCPOM, and fuel blends at different engine speeds and loads. Since RCPOM and fuel blends have LHVs than those of diesel, they have higher BSFC, and hence, the engine spends more fuel to maintain the same level of P_b as compared to diesel when the speed is increased.[72,72] The BSFC increased when the proportion of biodiesel in the mixture was higher. The D10RM80E10 blend had the lowest LHV, affording it the highest BSFC. This is because the maximum biodiesel content in the fuel was very high, affording the fuel with the highest BSFC. Moreover, the high density and viscosity of biodiesel during the fuel injection in the combustion chamber created larger droplets and inhibited evaporation, leading to an increase in BSFCs.[73] The increase in oxygen content after adding ethanol, on the other hand, increased the BSFC because ethanol has a lower calorific value, as reported by de Oliveira et al.[33] and Bhat et al.[74] At 50 and 75% engine load, the BSFC of the fuel blend did not vary much from that of biodiesel as the fuel blend had a calorific value similar to biodiesel. At a 25% engine load and 2300 rpm, the BSFCs of RCPOM, D40RM50E10, D30RM60E10, D20RM70E10, and D10RM80E10 were 22.54, 26.61, 28.81, 28.81, and 30.51% higher than those of diesel, respectively. At a 50% engine load, the BSFC of RCPOM was 22.89% higher than that of diesel at 2300 rpm. Unfortunately, there are no results from BSFC of all

https://doi.org/10.1021/acsomega.2c07537
ACS Omega 2023, 8, 9275−9290

fuel blends at 2300 rpm. When over 15% ethanol is added to the fuel blend, the engine cannot operate smoothly due to ignition failure, especially at high speeds. Because of the high concentration of ethanol in the mixture, there is a delay in ignition and automated ignition.[75] Consequently, there are no reports on the performance and emissions of D40RM50E10, D30RM60E10, D20RM70E10, and D10RM80E10 blends at a 50% engine load and 2300 rpm. Therefore, the BSFC of fuel blends reported in this study is at a maximum engine speed of 2000 rpm. The BSFCs of D40RM50E10, D30RM60E10, D20RM70E10, and D10RM80E10 were 14.46, 16.87, 20.48, and 21.69% higher than those of diesel, respectively. For a 75% engine load, the BSFC of RCPOM was 11.64% higher than that of diesel at 2300 rpm. Compared to diesel, the BSFCs of D40RM50E10, D30RM60E10, D20RM70E10, and D10RM80E10 were greater. The BSFCs were found to be 16.94, 12.55, 14.39, and 18.02%, for 2000, 1700, 1700, and 1200 rpm, respectively.

3.4.3. Brake Thermal Efficiency. The fuel efficiency of the diesel engine is explained by the effect of the BTE. The BTE is the ratio of the P_b received by the crankshaft of the engine to the energy supplied by the fuel to the engine.[76] The BTEs for all fuels at various engine speeds and loads are shown in Figure 5c. At a 25% engine load, the BTE for RCPOM was similar to that of diesel at all engine speeds. The BTEs for the fuel blends were comparable to those of diesel at low speeds of 1100−1700 rpm, and BTEs were lower than those of diesel as the speed of engine increased. At a 25% engine load, the BTEs for RCPOM, D40RM50E10, D30RM60E10, D20RM70E10, and D10RM80E10 at 2300 rpm were 4.19, 9.64, 9.66, 8.07, and 7.64% lower than that of diesel, respectively. At a 50% engine load, the BTEs for RCPOM, D40RM50E10, D30RM60E10, D20RM70E10, and D10RM80E10 were 4.46, 0.05, 0.42, 1.71, and 0.95% lower than BTEs for diesel at 2300, 2300, 2000, 2000, and 2000 rpm, respectively. Because biodiesel and ethanol have a lower LHV than diesel, they showed poorer combustion; hence, doubling the amount of biodiesel and ethanol in the blend considerably reduced the BTE.[32] Silitonga et al.[77] reported a similar result. A higher latent heat of vaporization of ethanol was shown to cause heat loss, which in turn reduced BTE. Additionally, the lower cetane number of ethanol resulted in a longer ignition delay, causing incomplete combustion of fuel and lower BTE. At a 75% engine load, the BTEs for all fuels were higher than diesel. At 2300 rpm, the BTE for RCPOM was 5.17% higher than that of diesel. The LHV and greater viscosity of biodiesel increased as the engine load increased and the cylinder temperature increased. Because of the increased spray characteristics of the fuel, this resulted in complete combustion in the chamber. Therefore, the BTE was improved.[78] The BTEs for D40RM50E10, D30RM60E10, D20RM70E10, and D10RM80E10 blends were higher than 2.17, 3.40, 3.52, and 2.13% at 2000, 1700, 1700, and 1400 rpm, respectively. Adding alcohol increased the BTE for fuel blends at high engine loads, which increased the oxygen level in blends. Because ethanol has a lower boiling point than diesel, less heat is lost during combustion when more oxygen is present in the fuel.[73] Theinnoi et al.[67] reported a similar result. They concluded that the O_2 content in ethanol improves the fuel combustion efficiency. Additionally, the low viscosity and surface tension of ethanol result in a better fuel spray and smaller droplet sizes, which improve the homogeneity of the mixing process. Taib et al.[79] reported that the water in biofuels evaporates during combustion, increasing the BTE of the engine. This is due to a decrease in combustion temperature and a decrease in the heating value of the fuel.

3.5. Engine Emission. *3.5.1. Exhaust Gas Temperature.* Figure 6a shows the exhaust gas temperature (EGT) of all fuels at different loads and speeds of engine. In all cases, the EGT increased as the load and speed increased. While the engine was operating under a higher load, it sprayed more fuel for combustion than under normal conditions. This increased the temperature in the cylinder, which increased the EGT.[73] The EGT of RCPOM was lower than that of diesel for all speeds at a 25% engine load. However, EGT levels for fuel blends were higher than those for diesel all engine speeds at 25% load. The EGT of RCPOM was 4.90% lower than that of diesel at 2300 rpm, the highest speed of the engine. Unlike diesel, biodiesel has a lower LHV, which means that it generates lower combustion chamber temperatures.[80] Therefore, biodiesel has a lower EGT than that of diesel, whereas the EGTs of D40RM50E10, D30RM60E10, D20RM70E10, and D10RM80E10 blends were 1.63, 0.92, 1.86, and 0.94% higher than that of diesel, respectively. When compared to diesel, the shorter combustion time of the fuel blend results in a modest increase in the EGT. Tan et al.[32] and Yilmaz et al.[73] reported similar results. They found that the low cetane number of alcohol led to a greater EGT due to a longer ignition delay. Moreover, the high oxygen content in alcohol contributed to higher combustion chamber temperatures and EGT. For an engine load of 50%, the EGTs of RCPOM were slightly higher than those of diesel at all speeds. At 2300 rpm, i.e., the engine maximum speed, the EGT of RCPOM was 5.17% higher than that of diesel. EGTs from fuel blends were higher than diesel at 1100−1400 rpm and lower than diesel at 1700−2000 rpm, except for the D40RM50E10 blend. The EGT of D40RM50E10 increased by 8.61% at 2000 rpm, while that of D30RM60E10, D20RM70E10, and D10RM80E10 decreased by 1.30, 6.81, and 7.50% at 1700 rpm, respectively, compared to diesel. At a 75% maximum load, the EGT of RCPOM was 1.83% lower than that of diesel at 2300 rpm. The EGTs of D40RM50E10 and D30RM60E10 were 9.87 and 4.49% higher than diesel at 2000 and 1700 rpm, respectively. Alternatively, the EGT of D20RM70E10 and D10RM80E10 blends was 7.68 and 2.7% lower than diesel at 1700 and 1400 rpm, respectively. A higher proportion of biodiesel in the diesohol lowered the EGT due to the low cetane number and LHV of biodiesel.[32] Additionally, increasing the amount of ethanol in the mixture led to a decrease in EGT because of increased latent heat of vaporization and decreased LHV of ethanol.[33,81]

3.5.2. Nitrogen Oxide Emissions. NO_x emissions are the primary pollutants emitted during the combustion of fuel in diesel engines, and NO_x causes climatic impacts as well as health concerns.[34] NO_x emissions are influenced by various factors of the fuel, including the air−fuel interaction in combustion, the combustion temperature in the cylinder, residence time, density, cetane number, and oxygen content.[29,74,77] Figure 6b shows the NO_x emissions for diesel, RCPOM, and fuel blends at various engine speeds and loads. The NO_x emission increased as the engine load increased.[74] The concentration of O_2 in the fuel is an important factor in NO_x emission, and high O_2 concentrations in biodiesel increase combustion, resulting in greater NO_x emissions, similar to diesel, as reported by Ramalingam and Rajendran[76] and Ghadikolaei et al.[80] Additionally, the higher viscosity factor of biodiesel results in the spraying of larger fuel droplets and an ignition delay, resulting in higher NO_x emissions, similar to those described by Altaie et al.[81] At a

https://doi.org/10.1021/acsomega.2c07537
ACS Omega 2023, 8, 9275−9290

speed of 2300 rpm, NO_x emissions from RCPOM combustion were 7.75, 13.18, and 15.94% higher than diesel at 25, 50, and 75% engine loads, respectively. For a 25% engine load, the NO_x emissions of fuel blends were lower than diesel at all engine speeds. The NO_x emissions of D40RM50E10, D30RM60E10, D20RM70E10, and D10RM80E10 were 19.94, 17.88, 24.06, and 26.69% lower than diesel at 2300 rpm, respectively, i.e., the maximum engine speed. At 50 and 75% engine loads, the NO_x emissions from fuel blends were higher than diesel when the engine speed was 1100−1400 rpm and lower than diesel when the engine speed was 1700−2000 rpm. At a 50% engine load, the NO_x emissions of D40RM50E10, D30RM60E10, D20RM70E10, and D10RM80E10 were 14.26, 16.93, 17.72, and 14.10% lower than diesel at 2000 rpm, respectively. At a 75% engine load, NO_x emissions of D40RM50E10, D30RM60E10, and D20RM70E10 were 32.44, 11.07, and 21.43% lower than diesel at 2000, 1700, and 1700 rpm, respectively. High NO_x emissions were observed when the concentration of biodiesel blends in diesohol was increased. According to studies by Jia et al.[70] and Zhang et al.,[78] NO_x emissions increase with the biodiesel content of the fuel blends. In particular, NO_x emissions of pure biodiesel were higher than those of diesel. However, adding ethanol to the mixture lowered the cetane number, leading in a longer ignition delay and increased NO_x levels at low speeds. Conversely, at high engine speeds, the high latent heat of vaporization and low heating value of ethanol result in lower NO_x formation.[34,70] Yilmaz et al.[73] and Ghadikolaei et al.[80] found a similar result, indicating that increased latent heat of alcohol vaporization is a critical factor contributing to heat absorption in the combustion chamber and the decrease in NO_x formation.

3.5.3. Carbon Monoxide and Carbon Dioxide Emissions. CO is a toxic, odorless, and colorless gas that causes air pollution. An insufficient oxygen content during the combustion of fuel in diesel engines causes incomplete combustion, leading to oxidation reactions that form CO.[16] Additionally, CO emissions depend on the physical and chemical properties of the fuel, fuel spraying characteristics, residence time, combustion chamber temperature, and air−fuel ratio.[82] Figure 6c shows the CO emissions of all fuels at different engine speeds for 25, 50, and 75% engine loads. At all loads, the higher oxygen content in biodiesel than diesel promoted better combustion, resulting in lower CO emissions than diesel.[82] The addition of biodiesel and ethanol to diesel reduced CO emissions because both fuels were oxygen-rich, enabling complete combustion of the fuel, and CO emissions of the fuel blend were significantly lower at higher engine loads. Subbaiah et al.[17] and Theinnoi et al.[67] reported a similar result. They concluded that the higher oxygen content of diesel−biodiesel−ethanol had a significant impact on CO reduction at higher engine loads. For a 25% engine load and 2300 rpm, the CO emissions from RCPOM, D40RM50E10, D30RM60E10, D20RM70E10, and D10RM80E10 were 19.07, 6.31, 6.05, 13.89, and 20.84% lower than diesel, respectively. At a 50% engine load, CO emissions from RCPOM were 12.82% lower than diesel at 2300 rpm. The CO emissions for fuel blends were lower than diesel, except for D40RM50E10 blend. The CO emissions of D40RM50E10 increased by 7.79%, whereas those of D30RM60E10, D20RM70E10, and D10RM80E10 decreased by 7.79, 9.15, and 15.33% at 2000 rpm, respectively, compared to diesel. For a 75% engine load, the CO emissions of RCPOM were 19.28% lower than diesel at 2300 rpm. For all fuel blends, the CO emissions of D40RM50E10, D30RM60E10, and D20RM70E10 were 39.16, 54.41, and 60.67% lower than diesel at 2000, 1700, and 1700 rpm, respectively, while those of D10RM80E10 were 9.21% higher than diesel at 1400 rpm. Because of the low calorific value and latent heat of ethanol addition, combustion temperatures were lower, resulting in CO emissions.[28] CO_2 is produced as a result of complete fuel combustion inside the cylinder. An increase in CO_2 shows higher complete combustion efficiency. Figure 6d shows the CO_2 emissions of different fuels at engine loads of 25, 50, and 75%. In general, CO_2 emissions increase with increased engine speed and load.[32] For engines at high speeds and loads, the high fuel consumption is used to burn without excess air, resulting in accelerated CO_2 formation.[34] At an engine speed of 2300 rpm, CO_2 emissions of RCPOM were 1.25, 2.28, and 2.29% higher than diesel at 25, 50, and 75% engine loads, respectively. The D40RM50E10 blend had the highest CO_2 emissions. However, all fuel blends had greater emissions than diesel. As a result of adding ethanol to the mixture, the D40RM50E10 blend had higher CO_2 emissions, indicating that more fuel combustion occurs than fuel oxidation, and CO_2 was released as a substitute for CO.[67] Subbaiah et al.[17] reported similar results and concluded that addition of ethanol in fuel affords higher CO_2 emissions. At a 25% engine load and 2300 rpm, the CO_2 emissions from D40RM50E10, D30RM60E10, D20RM70E10, and D10RM80E10 blends were 6.46, 1.65, 0.95, and 1.59% higher than diesel, respectively. At a 50% engine load and 2000 rpm, CO_2 emissions of D40RM50E10, D30RM60E10, D20RM70E10, and D10RM80E10 blends were 19.26, 8.13, 4.00, and 2.30% higher than diesel, respectively. At a 75% engine load, CO_2 from D40RM50E10, D30RM60E10, D20RM70E10, and D10RM80E10 blends were 8.86, 11.61, 1.91, and 14.00% higher than diesel at 2000, 1700, 1700, and 1400 rpm, respectively. The emissions of diesel and diesel blended with various proportions of biodiesel were analyzed by Chuah et al.[69] They reported that the biodiesel blend emitted more carbon dioxide than regular diesel because inefficient combustion occurred, and a lot of CO was turned into CO_2 because oxygen in the mixture reacted with the carbon atoms, causing the fuel to burn for a longer period.

3.5.4. Oxygen Gas. The amount of O_2 in exhaust gas is a measure of the combustion quality. A low O_2 content in the exhaust gas indicates complete combustion because O_2 is used to convert CO to CO_2 during the combustion process.[69] Figure 6e shows the emission of O_2 gas from all fuels in the exhaust gas. For all fuels, O_2 gas content decreases as the engine load increases. According to Ağbulut et al.,[83] the engine has a high volumetric efficiency at low engine speeds, which increases the O_2 content of fuels. As the engine speed increases, the flow of turbulent air in the chamber increases, which enhances the performance of the fuel blend. As a result, as the combustion quality improves, O_2 consumption increases, reducing the amount of excess O_2 released into the environment. The O_2 gas of RCPOM was lower than that of diesel fuel at almost all speeds. At a speed of 2300 rpm, the O_2 gas of RCPOM was 0.36, 1.00, and 1.5% lower than diesel at 25, 50, and 75% engine loads, respectively. For all fuel blends, the D40RM50E10 blend had the lowest O_2 gas in the fuel blends. The addition of ethanol results in the presence of a significant amount of O_2 in the mixture, which increased combustion and reduced O_2 gas content in the exhaust gas.[84] At a 25% engine load and 2300 rpm, O_2 from D40RM50E10 and D30RM60E10 was 1.76 and 0.80% lower than diesel, while those from D20RM70E10 and D10RM80E10 were 1.43 and 1.05% higher than diesel, respectively. At a 50% engine load at 2000 rpm, the O_2 gas of D40RM50E10 and

https://doi.org/10.1021/acsomega.2c07537
ACS Omega 2023, 8, 9275−9290

D30RM60E10 was 7.19 and 2.90% lower than diesel, while that of D20RM70E10 and D10RM80E10 was 4.52 and 1.95% higher than diesel, respectively. With a 75% engine load, the O_2 gas of D40RM50E10 and D30RM60E10 was 6.11 and 5.86% lower than diesel at 2000 and 1700 rpm, while the O_2 gas of D20RM70E10 and D10RM80E10 was 6.68 and 3.33% higher than diesel at 1700 and 1400 rpm, respectively.

3.5.5. Hydrocarbon Emissions. The factors that affect HC emissions are fuel properties, operating conditions, air−fuel ratio, fuel spraying, flame quenching, and fuel trapping in the crevices during combustion.[73] Figure 6f shows the HC emissions of all fuels as the engine speed and load increase. For all fuels, the results showed that HC emissions increased as the load increased. The HC emissions from RCPOM and fuel blends were lower than diesel at low loads, and HC emissions of RCPOM and fuel blends were higher than diesel at medium and high loads. At a 25% engine load at 2300 rpm, HC emissions from RCPOM were 32.21% lower than diesel. At 50 and 75% engine loads, the HC emissions of RCPOM were 29.50 and 46.81% higher than diesel at an engine speed of 2300 rpm, respectively. At a 25% engine load, the HC emissions of D40RM50E10, D30RM60E10, D20RM70E10, and D10RM80E10 were 16.83, 16.67, 27.88, and 16.35% lower than diesel at 2300 rpm, respectively. At a 50% engine load and 2000 rpm, HC emissions from D40RM50E10 were 9.62% lower than diesel, while those of D30RM60E10, D20RM70E10, and D10RM80E10 were 13.78, 3.85, and 5.77% higher than diesel, respectively. At a 75% engine load, the HC emissions of D40RM50E10, D30RM60E10, and D20RM70E10 were 16.75, 11.11, and 28.40% lower than diesel at 2000, 1700, and 1700 rpm, respectively, while that of D10RM80E10 was 50.72% higher than diesel at 1400 rpm. The results of this test were mostly related to the latent heat of ethanol, carbon−carbon double bond in biodiesel, and the physical and chemical nature of oxygen in ethanol and biodiesel, which led to lower HC emissions.[70] According to Jamrozik et al.,[27] a lower ethanol content decreases the viscosity and density of the mixture, resulting in better spraying and atomization, which leads to enhanced combustion and lower HC emissions. However, partially unburned ethanol, long-period combustion, a low cetane number, and a low cylinder temperature all contribute to greater HC emissions for some fuel blends.[84]

4. CONCLUSIONS

RCPOM from RCPO was successfully produced by the RSM technique with batch process transesterification reactions using commercial and community standards for agricultural diesel engines. RCPOM acted as an emulsifier in the blending process of diesel−hydrous ethanol fuels, enabling better fuel blending. The properties and phase stability of diesel−RCPOM−ethanol were investigated with a ternary diagram that corresponds to some requirements in the diesel standard. In addition, emissions and performance of RCPOM and fuel blends were tested and compared with those of diesel in an unmodified agricultural diesel engine at different speeds and loads of engines. The following are the conclusions of this study.

1. Under optimum conditions of 18.2 vol % methanol, 10.0 g/L KOH, a stirrer speed of 380 rpm, a reaction time of 36.4 min, and a reaction temperature of 60 °C, the batch transesterification process can produce ME with a purity of 96.91 wt % for RCPOM.
2. A ternary diagram was used to investigate the phase stability of diesel−RCPOM−hydrous ethanol blends at 35 °C (room temperature). A clear liquid single phase was observed when the concentration of RCPOM was >50 vol % and the concentration of diesel was <40 vol %. However, single-phase fuel blends were subject to some requirements according to the diesel standards, and therefore, only four fuel blends were used for performance and emission studies.
3. As concluded from the testing of performance of all fuels in diesel engines, the P_b of RCPOM is slightly lower than that of diesel at engine speeds of 1100−2300 rpm. The P_b of fuel blends increased as the engine speed increased from 1100 to 2000 rpm and decreased as the engine speed increased from 2000 to 2300 rpm because the cetane number of ethanol is lower than diesel. Moreover, BSFCs from RCPOM and fuel blends under all conditions were higher than those of diesel. The effect of BSFCs increases as the biodiesel concentration in the mixture increases, with the D10RM80E10 blended fuel having the highest BSFC. Due to a longer ignition delay, RCPOM and fuel blends had lower BTEs than diesel at 25 and 50% loads, but RCPOM had higher BTEs than diesel at the maximum load. The results also showed that adding alcohol to the mixture increased the oxygen level of the mixture, resulting in complete combustion of the fuel in the cylinder.
4. RCPOM had higher NO_x emissions than diesel in all cases. Because of the high latent heat of ethanol vaporization and LHV, NO_x emissions from fuel blends were lower than diesel at 50 and 75% loads, especially for the D40RM50E10 blend. Under all engine loads, RCPOM had lower CO emissions than diesel. Because both biodiesel and ethanol have high oxygen contents, they promote higher levels of combustion and therefore minimize CO emissions. All fuels had greater CO_2 emissions than diesel, with the D40RM50E10 blend having full combustion and the highest CO_2 emissions. Because complete combustion resulted in lower O_2 in the exhaust, the O_2 gas of the D40RM50E10 blend was among the lowest of all fuel blends. The HC emissions of the D40RM50E10 fuel blend were closest to diesel in all loads.

In unmodified diesel engines, the emissions and performance of fuel blends consisting of diesel−RCPOM−hydrous ethanol were tested. The fuel blend was simple to use in agricultural engines and required no engine modifications. Furthermore, this fuel blend could be used in diesel engine generators and water pumps. In this test, the D40RM50E10 blend was the most suitable fuel blend as it had the closest performance to diesel and the lowest environmental effect. According to the findings of this study, the D40RM50E10 blend performed admirably at an engine speed of 1700−2000 rpm and a 75% engine load. The complete combustion of the D40RM50E10 blend reduced NO_x and CO emissions by up to 32 and 55%, respectively, compared to diesel. Further research and development in the future can also examine the long-term effects of fuel blends on diesel engine components. It is also possible to investigate modified engines to change the fuel blend for maximum application efficiency.

https://doi.org/10.1021/acsomega.2c07537
ACS Omega 2023, 8, 9275−9290

AUTHOR INFORMATION

Corresponding Author

Krit Somnuk − *Department of Mechanical and Mechatronics Engineering, Faculty of Engineering, Prince of Songkla University, Hat Yai, Songkhla, Thailand 90110; Energy Technology Research Center, Faculty of Engineering, Prince of Songkla University, Hat Yai, Songkhla, Thailand 90110;* orcid.org/0000-0002-1771-5120; Email: krit.s@psu.ac.th

Authors

Jarernporn Thawornprasert − *Department of Mechanical and Mechatronics Engineering, Faculty of Engineering, Prince of Songkla University, Hat Yai, Songkhla, Thailand 90110*

Wiriya Duangsuwan − *Biotechnology Program, Center of Excellence in Innovative Biotechnology for Sustainable Utilization of Bioresourses, Faculty of Agro-Industry, Prince of Songkla University, Hat Yai, Songkhla, Thailand 90110*

Complete contact information is available at: https://pubs.acs.org/10.1021/acsomega.2c07537

Notes

The authors declare no competing financial interest.

ACKNOWLEDGMENTS

This work was supported by the Prince of Songkla University, Grant No. ENG6202045S, and the National Research Council of Thailand (NRCT), Grant No. NRCT5-RSA63022-04.

NOMENCLATURE

BSFC brake-specific fuel consumption
BTE brake thermal efficiency
CO carbon monoxide
CO_2 carbon dioxide
D40RM50E10 40 vol % diesel + 50 vol % RCPOM + 10 vol % ethanol blend
D30RM60E10 30 vol % diesel + 60 vol % RCPOM + 10 vol % ethanol blend
D20RM70E10 20 vol % diesel + 70 vol % RCPOM + 10 vol % ethanol blend
D10RM80E10 10 vol % diesel + 80 vol % RCPOM + 10 vol % ethanol blend
DG diglyceride
EGT exhaust gas temperature
FAME fatty acid methyl esters
FFA free fatty acid
HC hydrocarbon emissions
H_2SO_4 sulfuric acid
KOH potassium hydroxide
LHV lower heating value
RCPO refined crude palm oil
ERCPO esterified refined crude palm oil
RCPOM refined crude palm oil methyl ester
CPO crude palm oil
ME methyl ester
MG monoglyceride
NO_x nitrogen oxides
O_2 oxygen gas
P_b brake power
PM particulate matter
RSM response surface methodology
TG triglyceride
TLC/FID thin-layer chromatograph with flame ionization detector
vol % percentage by volume
wt % percentage by weight

REFERENCES

(1) The Business Research Company. Oil And Gas Global Market Report 2022 − By Type (Oil & Gas Upstream Activities, Oil Downstream Products), By Drilling Type (Offshore, Onshore), By Application (Residential, Commercial, Institutions) − Market Size, Trends, And Global Forecast 2022-2026 Home Page. https://www.thebusinessresearchcompany.com/report/oil-and-gas-global-market-report (accessed October 30, 2022).

(2) Pidol, L.; Lecointe, B.; Starck, L.; Jeuland, N. Ethanol−biodiesel−diesel fuel blends: Performances and emissions in conventional diesel and advanced low temperature combustions. *Fuel* **2012**, *93*, 329−338.

(3) Prasad, S.; Dhanya, M. S. Air Quality and Biofuels. In *Environmental Impact of Biofuels*; InTech, 2011.

(4) Bangjang, T.; Kaewchada, A.; Jaree, A. Modified diesohol using distilled cashew nut shell liquid and biodiesel. *Energy Fuels* **2016**, *30*, 8252−8259.

(5) Srinivasnaik, M.; Sudhakar, T. V. V.; Balunaik, B.; SomiReddy, A. Alcohols as Alternative Fuels for Diesel Engines: A Review. *Int. J. Appl. Sci. Technol.* **2015**, *3*, 1−8.

(6) Balat, M.; Balat, H. Recent trends in global production and utilization of bio−ethanol fuel. *Appl. Energy* **2009**, *86*, 2273−2282.

(7) Saxena, R. C.; Adhikari, D. K.; Goyal, H. B. Biomass−based energy fuel through biochemical routes: A review. *Renewable Sustainable Energy Rev.* **2009**, *13*, 167−178.

(8) Somnuk, K.; Soysuwan, N.; Prateepchaikul, G. Continuous process for biodiesel production from palm fatty acid distillate (PFAD) using helical static mixers as reactors. *Renewable Energy* **2019**, *131*, 100−110.

(9) Kim, H. Y.; Ge, J. C.; Choi, N. J. Effects of ethanol−diesel on the combustion and emissions from a diesel engine at a low idle speed. *Appl. Sci.* **2020**, *10*, 4153.

(10) Guarieiro, L. L. N.; Guerreiro, E. T.; de, A.; Amparo, K. K.; dos, S.; Manera, V. B.; Regis, A. C. D.; Santos, A. G.; Ferreira, V. P.; Leão, D. J.; Torres, E. A.; de Andrade, J. B. Assessment of the use of oxygenated fuels on emissions and performance of a diesel engine. *Microchem. J.* **2014**, *117*, 94−99.

(11) Jeong, J.-s.; Jeon, H.; Ko, K.-m.; Chung, B.; Choi, G.-W. Production of anhydrous ethanol using various PSA (Pressure Swing Adsorption) processes in pilot plant. *Renewable Energy* **2012**, *42*, 41−45.

(12) Augoye, A.; Aleiferis, P.Characterization of flame development with hydrous and anhydrous ethanol fuels in a spark−ignition engine with direct injection and port injection systems. *SAE Technical Paper Series*, 2014, Vol. *1*, pp 1-14.

(13) Nour, M.; Kosaka, H.; Sato, S.; Bady, M.; Abdel-Rahman, A. K.; Uchida, K. Effect of ethanol/water blends addition on diesel fuel combustion in RCM and DI diesel engine. *Energy Convers. Manage.* **2017**, *149*, 228−243.

(14) Yahuza, I.; Dandakouta, H.; Ejilah, R. I.; Dasin, D. Y.; Farinwata, S. S. Exhaust emissions characterization of a single cylinder diesel engine fueled with biodiesel−ethanol−diesel blends. *Int. J. Energy Eng.* **2018**, *8*, 19−24.

(15) de Farias, M. S.; Schlosser, J. F.; Estrada, J. S.; Perin, G. F.; Martini, A. T. Emissions of an agricultural engine using blends of diesel and hydrous ethanol. *Semina: Cienc. Agrar.* **2019**, *40*, 7−16.

(16) Lei, J.; Bi, Y.; Shen, L. Performance and emission characteristics of diesel engine fueled with ethanol−diesel blends in different altitude regions. *J. Biomed. Biotechnol.* **2011**, *2011*, 1−10.

(17) Subbaiah, G. V.; Gopal, K. R.; Hussain, S. A.; Prasad, B. D.; Reddy, K. T. Rice bran oil biodiesel Subbaiah as an additive in diesel−ethanol blends for diesel engines. *Int. J. Res. Rev. Appl. Sci.* **2010**, *3*, 334−342.

(18) Shahir, S. A.; Masjuki, H. H.; Kalam, M. A.; Imran, A.; Fattah, I. M. R.; Sanjid, A. Feasibility of diesel−biodiesel−ethanol/bioethanol blend as existing CI engine fuel: An assessment of properties, material compatibility, safety and combustion. *Renewable Sustainable Energy Rev.* **2014**, *32*, 379−395.
(19) O'Malley, J.; Searle, S. Air quality impacts of biodiesel in the United States. *ICCT* **2021**, 1−36.
(20) Ogunkunle, O.; Ahmed, N. A. Overview of biodiesel combustion in mitigating the adverse impacts of engine emissions on the sustainable human−environment scenario. *Sustainability* **2021**, *13*, 5465.
(21) Reddy, S. N. K.; Wani, M. M. A Comprehensive review on effects of nanoparticles−antioxidant additives−biodiesel blends on performance and emissions of diesel engine. *Appl. Sci. Eng. Prog.* **2020**, *13*, 285−298.
(22) Khoobbakht, G.; Karimi, M.; Kheiralipour, K. Effects of biodiesel−ethanol−diesel blends on the performance indicators of a diesel engine: A study by response surface modeling. *Appl. Therm. Eng.* **2019**, *148*, 1385−1394.
(23) Jin, C.; Zhang, X.; Wang, X.; Xiang, Y.; Cui, X.; Yin, Z.; Sun, X.; Ji, J.; Wang, G.; Liu, H. Effects of polyoxymethylene dimethyl ethers on the solubility of ethanol/diesel and hydrous ethanol/diesel fuel blends. *Energy Sci. Eng.* **2019**, *7*, 2855−2865.
(24) Shrivastava, K.; Thipse, S. S.; Patil, I. D. The phase stability and solubility of diesel, biodiesel and ethanol blends−A review. *Int. J. Mech. Prod. Eng.* **2015**, *3*, 40−44.
(25) Srikanth, H. V.; Godiganur, S.; Manne, B.; Kumar, S. B. Niger seed oil biodiesel as an emulsifier in diesel−ethanol blends for compression ignition engine. *Renewable Energy* **2021**, *163*, 1467−1478.
(26) Kumar, P. S.; Kumari, N. P.; Sharma, A. K. Cut−off percentage of ethanol in diesel−biodiesel based fuel blends and analysis of emissions in four stroke−compression ignition engines. *Nat. Environ. Pollut. Technol.* **2021**, *20*, 619−624.
(27) Jamrozik, A.; Tutak, W.; Pyrc, M.; Sobiepański, M. Effect of diesel−biodiesel−ethanol blend on combustion, performance, and emissions characteristics on a direct injection diesel engine. *Therm. Sci.* **2017**, *21*, 591−604.
(28) Klajn, F. F.; Gurgacz, F.; Lenz, A. M.; Iacono, G. E. P.; de Souza, S. N. M.; Ferruzzi, Y. Comparison of the emissions and performance of ethanol−added diesel−biodiesel blends in a compression ignition engine with those of pure diesel. *Environ. Technol.* **2018**, *41*, 511−520.
(29) Krishna, S. M.; Salam, P. A.; Tongroon, M.; Chollacoop, N. Performance and emission assessment of optimally blended biodiesel−diesel−ethanol in diesel engine generator. *Appl. Therm. Eng.* **2019**, *155*, 525−533.
(30) Shamun, S.; Belgiorno, G.; Blasio, G. D.; Beatrice, C.; Tunér, M.; Tunestål, P. Performance and emissions of diesel−biodiesel−ethanol blends in a light duty compression ignition engine. *Appl. Therm. Eng.* **2018**, *145*, 444−452.
(31) Kaulani, S. A.; Latiff, Z. A.; Perang, M. R. M.; Said, M. F. M.; Hasan, M. F.Performance and emission of compression ignition (CI) engine using ethanol−diesel blending as a fuel. In *AIP Conference Proceedings*, 2019. DOI: 10.1063/1.5085962.
(32) Tan, Y. H.; Abdullah, M. O.; Nolasco-Hipolito, C.; Zauzi, N. S. A.; Abdullah, G. W. Engine performance and emissions characteristics of a diesel engine fueled with diesel−biodiesel−bioethanol emulsions. *Energy Convers. Manage.* **2017**, *132*, 54−64.
(33) de Oliveira, A.; Sodre, J. R.; Valente, O. S.Performance of a diesel engine operating with blends of diesel, biodiesel and ethanol in the lower specific fuel consumption range. In *25th SAE BRASIL International Congress and Display*, 2016.
(34) Freitas, E. S. d. C.; Guarieiro, L. L. N.; da Silva, M.V.I.; Amparo, K. K. d. S.; Machado, B. A. S.; Guerreiro, E. T. d. A.; de Jesus, J. F. C.; Torres, E. A. Emission and performance evaluation of a diesel engine using addition of ethanol to diesel/biodiesel fuel blend. *Energies* **2022**, *15*, 2988.
(35) Gaurav, A.; Dumas, S.; Mai, C. T. Q.; Ng, F. T. T. A kinetic model for a single step biodiesel production from a high free fatty acid (FFA) biodiesel feedstock over a solid heteropolyacid catalyst. *Green Energy Environ.* **2019**, *4*, 328−341.
(36) Patel, A.; Brahmkhatri, V.; Singh, N. Biodiesel production by esterification of free fatty acid over sulfated zirconia. *Renewable Energy* **2013**, *51*, 227−233.
(37) Somnuk, K.; Smithmaitrie, P.; Prateepchaikul, G. Two−stage continuous process of methyl ester from high free fatty acid mixed crude palm oil using static mixer coupled with high−intensity of ultrasound. *Energy Convers. Manage.* **2013**, *75*, 302−310.
(38) Kapor, N. Z. A.; Maniam, G. P.; Ab Rahim, M. H..; Yusoff, M. M. Palm fatty acid distillate as a potential source for biodiesel production-a review. *J. Cleaner Prod.* **2017**, *143*, 1−9.
(39) Estiasih, T.; Ahmadi, K. Bioactive compounds from palm fatty acid distillate and crude palm oil. *IOP Conf. Ser.: Earth Environ. Sci.* **2018**, *131*, No. 012016.
(40) ZERO and Rainforest Foundation Norway. Palm Fatty Acid Distillate (PFAD) in biofuels Home Page. https://quillbot.com/grammar-check?utm_medium=paid_search&utm_source=google&utm_campaign=paraphrase_developing_brand&campaign_type=search (accessed October 30 2022).
(41) Japir, A. A.-W.; Salimon, J.; Derawi, D.; Bahadi, M.; Yusop, M. R. Purification of high free fatty acid crude palm oil using molecular distillation. *Asian J. Chem.* **2016**, *28*, 2549−2554.
(42) Mancini, A.; Imperlini, E.; Nigro, E.; Montagnese, C.; Daniele, A.; Orrù, S.; Buono, P. Biological and nutritional properties of palm oil and palmitic acid: effects on health. *Molecules* **2015**, *20*, 17339−17361.
(43) Essien, N. M.; Ofem, O. E.; Bassey, S. C. Comparative physical characterization, physio−chemical and fatty acid composition of some edible vegetable oils. *J. Adv. Biol. Biotechnol.* **2014**, *1*, 30−39.
(44) Thawornprasert, J.; Duangsuwan, W.; Somnuk, K. Reduction of free fatty acid in low free fatty acid of mixed crude palm oil (LMCPO): optimization of esterification parameters. *Mater. Sci. Forum* **2021**, *1023*, 111−118.
(45) Pavlović, S.; Šelo, G.; Marinković, D.; Planinić, M.; Tišma, M.; Stanković, M. Transesterification of sunflower oil over waste chicken eggshell-based catalyst in a microreactor: an optimization study. *Micromachines* **2021**, *12*, 120.
(46) ASTM. ASTM D97−17b Standard Test Method for Pour Point of Petroleum Products; ASTM International: West Conshohocken, PA, 2017. https://www.astm.org/.
(47) ASTM. ASTM D2500−17a Standard Test Method for Cloud Point of Petroleum Products and Liquid Fuels; ASTM International: West Conshohocken, PA, 2018. https://www.astm.org/.
(48) European Committee for Standardization. EN 14103 Fat and Oil Derivatives − Fatty Acid Methyl Esters (FAME) − Determination of Ester and Linolenic Acid Methyl Ester Contents, 2011.
(49) European Committee for Standardization. EN 14105 Fat and Oil Derivatives − Fatty Acid Methyl Esters (FAME) − Determination of Free and Total Glycerol and Mono−, Di−, Triglyceride Contents; European Committee for Standardization; Austrian Standards Institute: Vienna, Austria, 2011.
(50) ASTM. ASTM D664−09 Standard Test Method for Acid Number of Petroleum Products by Potentiometric Titration; ASTM International: West Conshohocken, PA, 2009. https://www.astm.org/.
(51) European Committee for Standardization. EN 14110 Fat and Oil Derivatives − Fatty Acid Methyl Esters (FAME) − Determination of Methanol Content, 2003.
(52) ASTM. ASTM D93−16a. Standard Test Methods for Flash Point by Pensky−Martens Closed Cup Tester; ASTM International: West Conshohocken, PA, 2016. https://www.astm.org/.
(53) ASTM. ASTM D1298−12b Standard Test Method for Density, Relative Density, or API Gravity of Crude Petroleum and Liquid Petroleum Products by Hydrometer Method; ASTM International: West Conshohocken, PA, 2017. https://www.astm.org/.
(54) ASTM. ASTM D445−17a Standard Test Method for Kinematic Viscosity of Transparent and Opaque Liquids (and Calculation of Dynamic Viscosity); ASTM International: West Conshohocken, PA, 2017. https://www.astm.org/.
(55) ISO. EN ISO 12937 ISO Standard Petroleum Products − Determination of Water − Coulometric Karl Fischer Titration Method;

https://doi.org/10.1021/acsomega.2c07537
ACS Omega 2023, 8, 9275−9290

International Organization for Standardization: Geneva, Switzerland, 2000.
(56) ASTM. ASTM E203−96 Standard Test Method for Water Using Volumetric Karl Fischer Titration; ASTM International: West Conshohocken, PA, 2017. https://www.astm.org/.
(57) ASTM. ASTM D130−04 Standard Test Method for Corrosiveness to Copper from Petroleum Products by Copper Strip Test; ASTM International: West Conshohocken, PA, 2004. https://www.astm.org/.
(58) ASTM. ASTM D4530−15 Standard Test Method for Determination of Carbon Residue (Micro Method); ASTM International: West Conshohocken, PA, 2015. https://www.astm.org/.
(59) European Committee for Standardization. EN 14111 Fat and Oil Derivatives − Fatty Acid Methyl Esters (FAME) − Determination of Iodine Value, 2003.
(60) ASTM. ASTM D2622−21 Standard Test Method for Sulfur in Petroleum Products by Wavelength Dispersive X−ray Fluorescence Spectrometry; ASTM International: West Conshohocken, PA, 2022. https://www.astm.org/.
(61) European Committee for Standardization. EN 14107 Fat and Oil Derivatives − Fatty Acid Methyl Esters (FAME) − Determination of Phosphorus Content by Inductively Coupled Plasma (ICP) Emission Spectrometry, 2003.
(62) ASTM. ASTM D874−13a Standard Test Method for Sulfated Ash from Lubricating Oils and Additives; ASTM International: West Conshohocken, PA, 2018. https://www.astm.org/.
(63) Sajjadi, B.; Raman, A. A. A.; Arandiyan, H. A Comprehensive Review on Properties of Edible and Non−Edible Vegetable Oil−Based Biodiesel: Composition, Specifications and Prediction Models. *Renewable Sustainable Energy Rev.* **2016**, *63*, 62−92.
(64) Atmanli, A.; Ileri, E.; Yilmaz, N. Optimization of Diesel−Butanol−Vegetable Oil Blend Ratios Based on Engine Operating Parameters. *Energy* **2016**, *96*, 569−580.
(65) Chang, A. S.; Sherazi, S. T. H.; Kandhro, A. A.; Mahesar, S. A.; Chang, F.; Shah, S. N.; Laghari, Z. H.; Panhwar, T. Characterization of Palm Fatty Acid Distillate of Different Oil Processing Industries of Pakistan. *J. Oleo. Sci.* **2016**, *65*, 897−901.
(66) Mahmudul, H. M.; Hagos, F. Y.; Mukhtar N A, M.; Mamat, R.; Abdullah, A. A. Effect of Alcohol on Diesel Engine Combustion Operating with Biodiesel−Diesel Blend at Idling Conditions. *IOP Conf. Ser. Mater. Sci. Eng.* **2018**, *318*, 1−9.
(67) Theinnoi, K.; Sawatmongkhon, B.; Wongchang, T.; Haoharn, C.; Wongkhorsub, C.; Sukjit, E. Effects of diesel−biodiesel−ethanol fuel blend on a passive mode of selective catalytic reduction to reduce NO_x emission from real diesel engine exhaust gas. *ACS Omega* **2021**, *6*, 27443−27453.
(68) Department of energy business, Ministry of energy. Determine the characteristics and quality of diesel fuel Home Page. http://elaw.doeb.go.th/document_doeb/TH/699TH_0001.pdf (accessed August 16, 2022).
(69) Chuah, L. F.; Aziz, A. R. A.; Yusup, S.; Bokhari, A.; Klemeš, J. J.; Abdullah, M. Z. Performance and emission of diesel engine fuelled by waste cooking oil methyl ester derived from palm olein using hydrodynamic cavitation. *Clean Technol. Environ. Policy* **2015**, *17*, 2229−2241.
(70) Jia, D.; Deng, X.; Lei, J. Analysis on the impact of biodiesel−ethanol−diesel fuel on the performance and emissions of a diesel engine. *Energy Sources, Part A* **2019**, *41*, 3013−3025.
(71) Tripathi, G.; Nag, S.; Dhar, A.; Patil, D. V. *Chapter 16: Fuel Injection Equipment (FIE) Design for the New-generation Alternative Fuel-powered Diesel Engines*; Springer: Singapore, 2018.
(72) Heydari-Maleney, K.; Taghizadeh-Alisaraei, A.; Ghobadian, B.; Abbaszadeh-Mayvan, A. Analyzing and evaluation of carbon nanotubes additives to diesohol−B2 fuels on performance and emission of diesel engines. *Fuel* **2017**, *196*, 110−123.
(73) Yilmaz, N.; Ileri, E.; Atmanli, A. Performance of biodiesel/higher alcohols blends in a diesel engine. *Int. J. Energy Res.* **2016**, *40*, 1134−1143.
(74) Bhat, S. N.; Shenoy, S.; Dinesha, P. Effect of bio−ethanol on the performance and emission of a biodiesel fueled compression ignition engine. *MATEC Web Conf.* **2018**, *144*, 04017.
(75) V, S.; Amirthagadeswaran, K. S. Combustion and performance characteristics of water−in−diesel emulsion fuel. *Energy Sources* **2015**, *37*, 2020−2028.
(76) Ramalingam, S.; Rajendran, S. Advances in Eco−Fuels for a Sustainable Environment ‖ Assessment of performance, combustion, and emission behavior of novel annona biodiesel−operated diesel engine. *Woodhead Publ. Ser. Energy* **2019**, 391−405.
(77) Silitonga, A. S.; Masjuki, H. H.; Ong, H. C.; Sebayang, A. H.; Dharma, S.; Kusumo, F.; Siswantoro, J.; Milano, J.; Daud, K.; Mahlia, T. M. I.; Chen, W. H.; Sugiyanto, B. Evaluation of the engine performance and exhaust emissions of biodiesel−bioethanol−diesel blends using kernel−based extreme learning machine. *Energy* **2018**, *159*, 1075−1087.
(78) Zhang, Y.; Zhong, Y.; Wang, J.; Tan, D.; Zhang, Z.; Yang, D. Effects of different biodiesel−diesel blend fuel on combustion and emission characteristics of a diesel engine. *Processes* **2021**, *9*, 1984.
(79) Taib, N. M.; Mansor, M. R. A.; Mahmood, W. M. F. W.; Shah, F. A.; Abdullah, N. R. N. Investigation of diesel−ethanol blended fuel properties with palm methyl ester as co−solvent and blends enhancer. *MATEC Web Conf.* **2017**, *90*, 01080.
(80) Ghadikolaei, M. A.; Cheung, C. S.; Yung, K.-F. Study of combustion, performance and emissions of diesel engine fueled with diesel/biodiesel/alcohol blends having the same oxygen concentration. *Energy* **2018**, *157*, 258−269.
(81) Altaie, M. A. H.; Janius, R. B.; Rashid, U.; Taufiq-Yap, Y. H.; Yunus, R.; Zakaria, R.; Adam, N. M. Performance and exhaust emission characteristics of direct−injection diesel engine fueled with enriched biodiesel. *Energy Convers. Manage.* **2015**, *106*, 365−372.
(82) Appavu, P.; Madhavan, V. R.; Venu, H.; Jayaraman, J. A novel alternative fuel mixture (diesel−biodiesel−pentanol) for the existing unmodified DI diesel engine: performance and emission characteristics. *Trans. Can. Soc. Mech. Eng.* **2020**, *44*, 1−9.
(83) Ağbulut, Ü.; Sarıdemir, S.; Albayrak, S. Experimental investigation of combustion, performance and emission characteristics of a diesel engine fuelled with diesel−biodiesel−alcohol blends. *J. Braz. Soc. Mech. Sci. Eng.* **2019**, *41*, No. 389.
(84) El-Sheekh, M. M.; Bedaiwy, M. Y.; El-Nagar, A. A.; ElKelawy, M.; Bastawissi, H. A.-E. Ethanol biofuel production and characteristics optimization from wheat straw hydrolysate: Performance and emission study of DI−diesel engine fueled with diesel/biodiesel/ethanol blends. *Renewable Energy* **2022**, *191*, 591−607.

https://doi.org/10.1021/acsomega.2c07537
ACS Omega 2023, 8, 9275−9290